

AperTO - Archivio Istituzionale Open Access dell'Università di Torino

Spatiotemporal optical dark X solitary waves

This is the author's manuscript

Original Citation:

Availability:

This version is available <http://hdl.handle.net/2318/1707350> since 2019-07-23T18:05:21Z

Published version:

DOI:10.1364/OL.41.005571

Terms of use:

Open Access

Anyone can freely access the full text of works made available as "Open Access". Works made available under a Creative Commons license can be used according to the terms and conditions of said license. Use of all other works requires consent of the right holder (author or publisher) if not exempted from copyright protection by the applicable law.

(Article begins on next page)

Spatiotemporal optical dark X solitary waves

FABIO BARONIO,^{1,*} SHIHUA CHEN,² MIGUEL ONORATO,^{3,4} STEFANO TRILLO,⁵
STEFAN WABNITZ,¹ AND YUJI KODAMA⁶

¹INO CNR and Dipartimento di Ingegneria dell'Informazione, Università di Brescia, Via Branze 38, 25123 Brescia, Italy

²Department of Physics, Southeast University, Nanjing 211189, China

³Dipartimento di Fisica, Università di Torino, Via P. Giuria 1, 10125 Torino, Italy

⁴Istituto Nazionale di Fisica Nucleare, INFN, Sezione di Torino, 10125 Torino, Italy

⁵Dipartimento di Ingegneria, Università di Ferrara, Via Saragat 1, 44122 Ferrara, Italy

⁶Department of Mathematics, Ohio State University, Columbus, Ohio 43210, USA

*Corresponding author: fabio.baronio@unibs.it

Received 29 August 2016; revised 25 October 2016; accepted 27 October 2016; posted 2 November 2016 (Doc. ID 274266);
published 29 November 2016

We introduce spatiotemporal optical dark X solitary waves of the $(2 + 1)$ D hyperbolic nonlinear Schrödinger equation (NLSE), which rules wave propagation in a self-focusing and normally dispersive medium. These analytical solutions are derived by exploiting the connection between the NLSE and a well-known equation of hydrodynamics, namely the type II Kadomtsev-Petviashvili (KP-II) equation. As a result, families of shallow water X soliton solutions of the KP-II equation are mapped into optical dark X solitary wave solutions of the NLSE. Numerical simulations show that optical dark X solitary waves may propagate for long distances (tens of nonlinear lengths) before they eventually break up, owing to the modulation instability of the continuous wave background. This finding opens a novel path for the excitation and control of X solitary waves in nonlinear optics. © 2016 Optical Society of America

OCIS codes: (190.0190) Nonlinear optics; (190.5940) Self-action effects; (190.3270) Kerr effect.

Laser pulse and beam shaping techniques [1] aiming to obtain localized distortionless (both nondiffractive and nondispersive) wave packets [2] are of paramount importance in many fields of basic and applied research such as atomic physics, spectroscopy, communications, and medicine. In this context, X waves, originally discovered in acoustics [3], have been established as a new paradigm in areas ranging from classical to quantum optics [4–11]. Specifically, envelope X waves emerged to be the key for understanding the dynamics in so-called bi-dispersive settings, e.g., the spatiotemporal dynamics ruled by standard paraxial diffraction in normally dispersive media. X waves exist in the linear regime [2,12,13], being non-monochromatic superpositions of nondiffracting modes (Bessel [14] or cosine modes in transverse two-dimensional [2D] and one-dimensional [1D], respectively). However, it is their *nonlinear* counterpart (obtained via numerical dressing of linear solutions [5,15]) that

attracted much interest because of their capability to emerge spontaneously in different experiments involving parametric converters [5,6], Kerr media [7,8], and periodic structures [10].

The nonlinear regime, however, poses a number of challenges that remained unaddressed to date. First, there are no available methods to construct analytical solutions. Exact nonlinear X wave solutions are known only in the presence of a potential which rules out the most interesting experimental situations that involve free propagation [16]. Second, only bright nonlinear X waves have been reported, whereas the possibility to find dark X waves over a finite background was largely overlooked.

In this Letter, we show that both restrictions can be overcome at once by exploiting a transformation [17–19] that maps the most universal of bidispersive nonlinear models, namely the $(2 + 1)$ D nonlinear Schrödinger equation (NLSE) into the $(2 + 1)$ D Kadomtsev-Petviashvili (KP) equation. The latter constitutes the natural extension of the well-known $(1 + 1)$ D Korteweg-de Vries (KdV) equation and is widely employed in plasma and hydrodynamics (see e.g., [20–25]) in its two different forms, the so-called KP-I type and KP-II type, depending on the sign of the transverse perturbation to the KdV equation. In particular, we first show how the original two-soliton X-shaped solutions [23] of the KP-II generate nonlinear dark X solitary solutions of the hyperbolic NLSE, which are potentially observable in the regime investigated experimentally in [6,8,10]. Then, we consider a different family of X soliton solutions of the KP-II equation, namely the *Toda-type* [23], and find their optical dark X solitary counterpart of the NLSE.

In the presence of group-velocity dispersion and 1D diffraction, the dimensionless time-dependent paraxial wave equation in cubic Kerr media reads as [5]

$$iu_z + \frac{\alpha}{2}u_{tt} + \frac{\beta}{2}u_{yy} + \gamma|u|^2u = 0, \quad (1)$$

namely, the $(2 + 1)$ D, or more precisely $(1 + 1 + 1)$ D, NLSE, where $u(t, y, z)$ stands for the complex wave envelope, and t, y represent the retarded time (in the frame traveling at

the natural group velocity) and the spatial transverse coordinate, respectively, and z is the longitudinal propagation coordinate. Each subscripted variable in Eq. (1) stands for partial differentiation. α, β, γ are real constants that describe the effect of dispersion, diffraction, and Kerr nonlinearity, respectively.

We refer to Eq. (1) as *elliptic* NLSE if $\alpha\beta > 0$, and *hyperbolic* NLSE if $\alpha\beta < 0$. In the case of weak nonlinearity, weak diffraction, and slow modulation, the dynamics of optical NLSE dark envelopes $u(t, y, z)$ may be related to the hydrodynamic KP variable $\eta(\tau, v, \varsigma)$ as follows [19]:

$$u(t, y, z) \simeq \sqrt{\rho_0 + \eta(\tau, v, \varsigma)} e^{[\gamma \rho_0 z - (\gamma/c_0) \int \eta(\tau, v, \varsigma) d\tau]}, \quad (2)$$

where ρ_0 stands for a background continuous wave amplitude, $\eta(\tau, v, \varsigma)$ represents a small amplitude variation, say $\eta \sim \mathcal{O}(\varepsilon)$ with $0 < \varepsilon \ll 1$ and the order one background ρ_0 ; $\eta(\tau, v, \varsigma)$ satisfies the KP equation

$$\left(-\eta_\varsigma + \frac{3\alpha\gamma}{2c_0} \eta \eta_\tau + \frac{\alpha^2}{8c_0} \eta_{\tau\tau} \right)_\tau - \frac{c_0\beta}{2\alpha} \eta_{vv} = 0, \quad (3)$$

where $\tau = t - c_0 z$, $v = y$, $\varsigma = z$ with $c_0 = \sqrt{-\gamma\alpha\rho_0}$, and $\alpha\gamma < 0$ (see [19] for further details).

In contrast to the case dealt with in [19], which considered lump solutions of the elliptic NLSE for defocusing media ($\alpha, \beta > 0, \gamma < 0$), derived through Eq. (2) from the KP-I equation [Eq. (3) with $\beta/\alpha > 0$], in this Letter we focus our attention on the combined action of diffraction and normal dispersion for self-focusing media. The latter case corresponds to $\alpha < 0$ and $\beta, \gamma > 0$, i.e., to the focusing hyperbolic NLSE linked through Eq. (2) to the KP-II equation [$\beta/\alpha < 0$ in Eq. (3)]. Interestingly, the results that we derive below have relevance also in different contexts where the same hyperbolic NLSE applies, such as the propagation in suitably engineered lattices giving rise to effective negative diffraction [10,26], or the dynamics of envelope water waves [27]. (In both cases, t represents an additional spatial variable.)

In order to proceed further we fix, without loss of generality, the coefficients of Eq. (1) as $\alpha = -4\sqrt{2}$, $\beta = 6\sqrt{2}$, $\gamma = 2\sqrt{2}$, and the background to unit $\rho_0 = 1$. On the one hand, this allows us to cast Eq. (3) in its standard KP-II form $(-\eta_\varsigma - 6\eta\eta_\tau + \eta_{\tau\tau})_\tau + 3\eta_{vv} = 0$. On the other hand, this fixes the scaling between the dimensionless variables z, t, y in Eq. (1) and the corresponding real-world quantities $Z = Z_0 z$, $T = T_0 t$, $Y = Y_0 y$. The longitudinal scaling factor turns out to be $Z_0 = 2\sqrt{2}L_{\text{nl}}$, where $L_{\text{nl}} = (\gamma_{\text{phys}} I_0)^{-1}$ is the usual nonlinear length associated with the intensity I_0 of the background and $\gamma_{\text{phys}} = k_0 n_{2l}$, n_{2l} being the Kerr nonlinear index and k_0 the vacuum wavenumber. The “transverse” scales read as $T_0 = \sqrt{k'' L_{\text{nl}}/2}$ and $Y_0 = \sqrt{L_{\text{nl}}/(3k_0 n)}$, where k'' and n are the group-velocity dispersion and the linear refractive index, respectively.

The KP-II equation admits complicated soliton solutions, mostly discovered in the last decade, which may describe non-trivial web patterns generated under resonances of line solitons observable in shallow water [23–25]. Among these, we first consider the so-called *O-type* bright X-shaped two-soliton solution of the KP-II. (Note that the name *O-type* is due to the fact that this solution was originally found by the Hirota bilinear method [23]; it should not be confused with the conical *O*-waves of the elliptic NLSE [2], which have no relevance in the present context.) When considering small amplitude

regimes, a formula for an exact *O-type* solution of Eq. (3) can be expressed as follows [23]:

$$\eta(\tau, v, \varsigma) = -2(\ln F)_{\tau\tau}, \quad (4)$$

where the function $F(\tau, v, \varsigma)$ is given by $F = f_1 + f_2$ with

$$f_1 = (\varepsilon_1 + \varepsilon_2) \cosh[(\varepsilon_1 - \varepsilon_2)\tau + 4(\varepsilon_1^3 - \varepsilon_2^3)\varsigma],$$

$$f_2 = 2\sqrt{\varepsilon_1 \varepsilon_2} \cosh[(\varepsilon_1^2 - \varepsilon_2^2)v].$$

$\varepsilon_1, \varepsilon_2$ are small real positive parameters which are related to the amplitude, width, and the angle of the *O-type* X-soliton solutions.

The expression of (2+1)D NLSE dark X solitary waves $u(t, y, z)$ is directly given through Eq. (2), exploiting the soliton expression for $\eta(\tau, v, \varsigma)$ in Eq. (4).

Figure 1 shows the spatiotemporal envelope intensity profile $|u|^2$ of a (2+1)D NLSE dark X solitary wave of the hyperbolic NLSE. The analytical solution is shown in the (y, t) plane, at $z = 0$ in Fig. 1(a) and at $z = 10$ in Fig. 1(b). In this particular example, we have chosen $\varepsilon_1 = 0.2$, $\varepsilon_2 = 0.001$. Specifically, Figs. 1(a) and 1(b) illustrate a solitary solution that describes the X-interaction of multiple dark line solitons. Asymptotically, the solution reduces to two line dark waves for $t \ll 0$ and two for $t \gg 0$, with intensity dips $\frac{1}{2}(\varepsilon_1 - \varepsilon_2)^2$ and characteristic angles $\pm \tan^{-1}(\varepsilon_1 + \varepsilon_2)$, measured from the y axis. The maximum value of the dip in the interaction region is $2(\varepsilon_1 - \varepsilon_2)^2(\varepsilon_1 + \varepsilon_2)/(\varepsilon_1 + \varepsilon_2 + 2\sqrt{\varepsilon_1 \varepsilon_2})$. Next, we numerically verified the accuracy and stability of the analytically predicted *O-type* dark X solitary wave of the NLSE. To this end, we made use of a standard split-step Fourier technique, commonly adopted in the numerical solution of the NLSE Eq. (1). We took the dark wave envelope at $z = 0$ as the numerical input: $u(t, y, z = 0) = \sqrt{1 + \eta(\tau = t, v = y, \varsigma = 0)} \exp[i\phi(\tau = t, v = y, \varsigma = 0)]$, where η is the X-soliton solution (4) and $\phi = -(\gamma/c_0) \int_\tau \eta$. Figure 1(c) shows the (y, t) profile of the numerical solution of the hyperbolic NLSE obtained at $z = 10$, which shows excellent agreement with the analytical solution from Eq. (4) computed at $z = 10$, and reported in Fig. 1(b). We estimate the error between the asymptotic formula and the X solitary wave in the numerics to be lower than 1%. These results prove that the proposed solutions propagate as X-shaped nonlinear invariant modes of the NLSE, being subject only to a net delay due to the deviation c_0 from the natural group velocity of the medium. The spatiotemporal Fourier spectrum of these waves is also X-shaped (result not shown). These features allow us to classify such waves in the broad class of diffraction-free and dispersion-free X waves. It is worth pointing out, however, that there are important differences with the more general nonlinear X wave solution reported in the literature for the (3+1)D hyperbolic NLSE, i.e., for 2D diffraction [5,15]. In particular, the latter type of X waves exhibits a characteristic decay $1/r$ along the spatial coordinate r which is characteristic of the Bessel functions constituting the building blocks of X waves in the linear limit. Conversely, in the present case, the dark X solitary waves have, by construction, a constant asymptotic (i.e., the line solitons), while the transformation in Eq. (2) becomes meaningless in the linear limit. Nevertheless, the asymptotic state is compatible with 1D transverse diffraction (see, e.g., Fig. 1 in [10]), a regime where the connections between the linear and nonlinear X-waves have not been exhaustively investigated yet. Of course, any finite energy realization of the

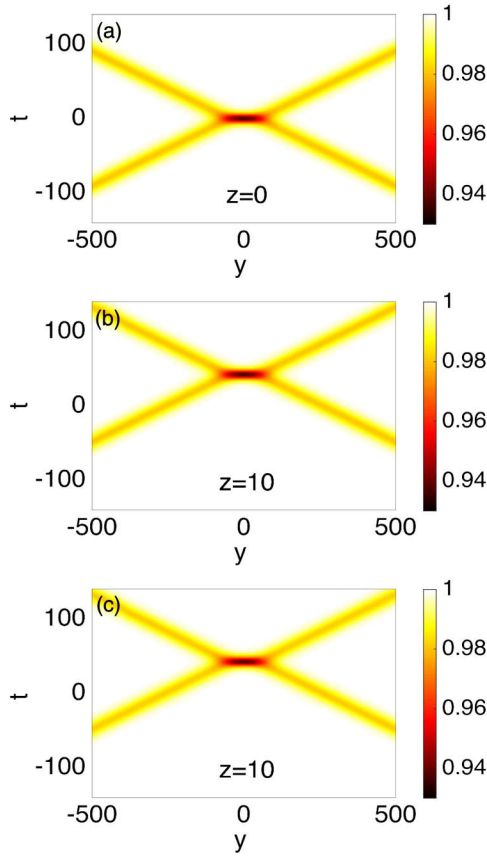


Fig. 1. Spatiotemporal NLSE envelope intensity distribution $|u|^2$, in the (y, t) plane, showing a typical dark X solitary wave. (a) $|u|^2$ at $z = 0$ and (b) at $z = 10$. (c) Numerically computed profile $|u|^2$ according to hyperbolic NLSE (1) at the propagation distance $z = 10$. Here, $\varepsilon_1 = 0.2$, $\varepsilon_2 = 0.001$.

present type of solutions should consider a spatiotemporal envelope modulation of the X solitary wave that decays to zero sufficiently slowly in (t, y) compared with the extension of the solitary central notch, similar to the case of dark solitons in $(1 + 1)$ D [28].

The link between the hyperbolic NLSE and the KP-II equation is not limited to the type of invariant waves discussed above. Among the variety of other types of KP-II X-shaped soliton solutions found in the last decade, e.g., so-called *T-type* and *P-type* soliton solutions [23], below we discuss the relevance of the *T-type* solitons. They originate from the soliton solutions found in the *Toda lattice* equation [29] and describe a fully resonant interaction of two line solitons. When considering the small amplitude regime, the exact *Toda-type* soliton solution of Eq. (3) can be expressed in the form

$$\eta(\tau, v, \zeta) = -2(\ln F)_{\tau\tau}, \quad (5)$$

where $F = f_1 + f_2$ with

$$\begin{aligned} f_1 &= (\varepsilon_1 + \varepsilon_2)^2 \cosh[(\varepsilon_1 - \varepsilon_2)\tau + 4(\varepsilon_1^3 - \varepsilon_2^3)\zeta], \\ f_2 &= 2(\varepsilon_1 - \varepsilon_2)\sqrt{\varepsilon_1\varepsilon_2}\{\cosh[(\varepsilon_1^2 - \varepsilon_2^2)v] \\ &\quad + \cosh[4(\varepsilon_1^3 + \varepsilon_2^3)\zeta + (\varepsilon_1 + \varepsilon_2)\tau]\}. \end{aligned}$$

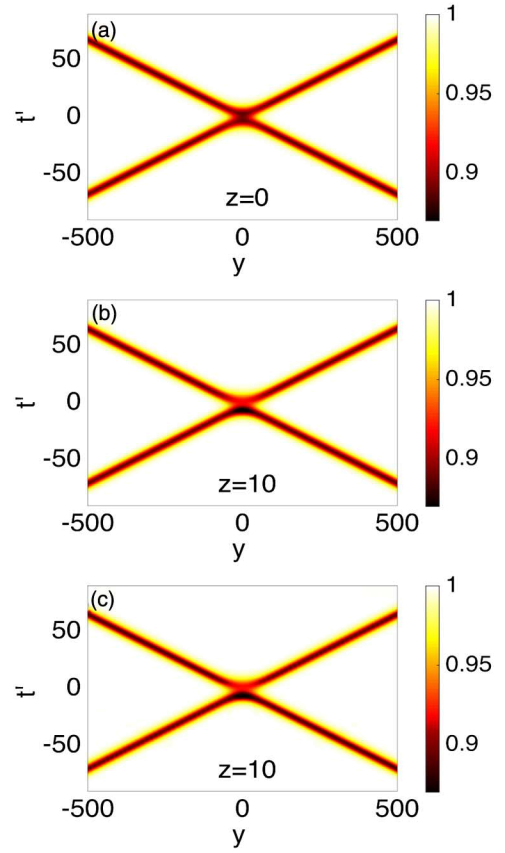


Fig. 2. Spatiotemporal NLSE envelope intensity distribution $|u|^2$, in the (y, t') plane ($t' = t - c_0 z$), showing a dark X solitary wave fission. (a) $|u|^2$ at $z = 0$ and (b) at $z = 10$. (c) Numerically computed profile $|u|^2$ at the propagation distance $z = 10$. Here, $\varepsilon_1 = 0.31$, $\varepsilon_2 = 0.17$.

$\varepsilon_1, \varepsilon_2$ are small real positive parameters that rule the amplitude, width, and angle of the *Toda-type* solution.

Again, the $(2 + 1)$ D NLSE dark X solitary waves $u(t, y, z)$ are directly obtained through Eq. (2), exploiting the soliton expression for $\eta(\tau, v, \zeta)$ in Eq. (5). Figure 2(a) shows the spatiotemporal envelope intensity profile $|u|^2$ of a $(2 + 1)$ D NLSE dark X solitary wave in the (y, t') plane at $z = 0$, while the same profile at $z = 10$ is shown Fig. 2(b). Here, $t' = t - c_0 z$ stands for the retarded time in the frame where the solitary wave is stationary, and we set $\varepsilon_1 = 0.31$ and $\varepsilon_2 = 0.17$.

In particular, Fig. 2(a) illustrates an exact X shape, formed at the intersection point on the origin, which is given by the sum of the dark line solitary waves. The solution has, asymptotically, two line dark waves for $t \ll 0$ and two for $t \gg 0$, with the intensity dip $\frac{1}{2}(\varepsilon_1 + \varepsilon_2)^2$ and the angles of $\pm \tan^{-1}(\varepsilon_1 - \varepsilon_2)$, measured from the y axis. Upon propagation, the initial X shape experiences a sort of a fission and generates a solitary notch at the intersection point. The observed amplification of the notch means that the initial waveform, which is given by the sum of two dark line solitary waves, creates a large dispersive perturbation at the intersection point, which opens in a resonant solitary box. Because of this distortion, the T-type dark X solitary wave cannot be considered as a strictly invariant wave. In order to check whether this behavior is fully reproduced in the NLSE dynamics, we report in Fig. 2(c) the outcome of the numerical

integration of the NLSE at $z = 10$. By comparing Figs. 2(b) and 2(c), we conclude that T-type analytical solutions provide an excellent approximation of the dynamics ruled by the hyperbolic NLSE. In this case, we estimate the error to be lower than 2%. Remarkably, the approach remains reasonably accurate, even for relatively strong modulations. For instance, for a modulation depth up to $0.5\rho_0$, the error remains lower than 8%.

Let us finally discuss the important issue of the stability of the predicted dark X solitary waves of the hyperbolic NLSE. Two instability factors may affect the propagation of these waves. The first one is the modulation instability (MI) of the continuous wave background. In the case considered here ($\alpha < 0$, β , $\gamma > 0$) MI is of the conical type [27,30,31]. Generally, MI can be advantageous to form bright X waves from completely different initial conditions, both in the absence [5] or in the presence [32] of the background. The second mechanism is related to the transverse instability of the line solitons that compose the asymptotic state of the dark X wave [33]. We point out that such instability is known to occur for the NLSE, despite the fact that line solitons are transversally stable in the framework of the KP-II (unlike those of the KP-I) [20]. However, in our simulations of the NLSE (we performed different runs for other values of the parameters), these transverse instabilities never appear, since they are extremely long range, especially for shallow solitons. In fact, we found that the primary mechanism that affects the stability of dark X solitary waves is the MI of the background. As a result, the onset of MI causes the distortion of the solitary waves due to the amplification of spatiotemporal frequencies which are outside the spatiotemporal soliton spectrum. However, typically, this occurs only after tens of nonlinear lengths, usually beyond the sample lengths employed in optical experiments. Indeed, the effect of MI becomes visible only for distances longer than those shown in Figs. 1 and 2, i.e., for $z > 10 - 20$, which correspond to real-world distances $Z > 30 - 60L_{nl}$.

In summary, we have predicted the existence of optical spatiotemporal dark X solitary waves in media described by the $(2 + 1)$ D hyperbolic NLSE, ruling the propagation in self-focusing and normally dispersive media. In particular, we have shown, analytically and numerically, the families of optical dark X solitary waves of the NLSE, derived from families of shallow water X wave solitons of the KP-II model. This finding opens a novel path for the excitation and control of X waves in nonlinear optics and in other areas where such NLSE applies (Bose-Einstein condensation, acoustics); in fact, the nonlinear dark X solitary wave solutions of the NLSE are potentially observable in the regimes investigated experimentally in [6,8,10] and in [34–36].

Funding. Italian Ministry of University and Research (MIUR) (2012BFNWZ2); National Natural Science Foundation of China (NSFC) (11174050, 11474051); National Science Foundation (NSF) (1410267).

REFERENCES

1. A. Forbes, *Laser Beam Propagation: Generation and Propagation of Customised Light* (CRC Press, 2014).
2. H. E. Hernández-Figueroa, E. Recami, and M. Zamboni-Rached, *Localized Waves* (Wiley, 2008).
3. J. Lu and J. F. Greenleaf, IEEE Trans. Ultrason. Ferroelectr. Freq. Control **39**, 19 (1992).
4. P. Saari and M. Ratsep, Phys. Rev. Lett. **79**, 4135 (1997).
5. C. Conti, S. Trillo, P. Di Trapani, G. Valiulis, A. Piskarskas, O. Jedrkiewicz, and J. Trull, Phys. Rev. Lett. **90**, 170406 (2003).
6. P. Di Trapani, G. Valiulis, A. Piskarskas, O. Jedrkiewicz, J. Trull, C. Conti, and S. Trillo, Phys. Rev. Lett. **91**, 093904 (2003).
7. M. Kolesik, E. M. Wright, and J. V. Moloney, Phys. Rev. Lett. **92**, 253901 (2004).
8. D. Faccio, M. A. Porras, A. Dubietis, F. Bragheri, A. Couairon, and P. Di Trapani, Phys. Rev. Lett. **96**, 193901 (2006).
9. A. Ciattoni and C. Conti, J. Opt. Soc. Am. B **24**, 2195 (2007).
10. Y. Lahini, E. Frumker, Y. Silberberg, S. Droulias, K. Hizanidis, R. Morandotti, and D. N. Christodoulides, Phys. Rev. Lett. **98**, 023901 (2007).
11. M. Omigotti, C. Conti, and A. Szameit, Phys. Rev. Lett. **115**, 100401 (2015).
12. M. A. Porras, C. Conti, S. Trillo, and P. Di Trapani, Opt. Lett. **28**, 1090 (2003).
13. D. N. Christodoulides, N. K. Efremidis, P. Di Trapani, and B. A. Malomed, Opt. Lett. **29**, 1446 (2004).
14. J. Durnin, J. J. Miceli, and J. H. Eberly, Phys. Rev. Lett. **58**, 1499 (1987).
15. R. W. Boyd, S. G. Lukishova, and Y. R. Shen, *Self-Focusing: Past and Present, Fundamentals and Prospects* (Springer, 2009).
16. N. K. Efremidis, G. A. Siviloglou, and D. N. Christodoulides, Phys. Lett. A **373**, 4073 (2009).
17. E. A. Kuznetsov and S. K. Turitsyn, Sov. Phys. JEPT **67**, 1583 (1988).
18. D. E. Pelinovsky, Y. A. Stepanyants, and Y. S. Kivshar, Phys. Rev. E **51**, 5016 (1995).
19. F. Baronio, S. Wabnitz, and Y. Kodama, Phys. Rev. Lett. **116**, 173901 (2016).
20. B. B. Kadomtsev and V. I. Petviashvili, Sov. Phys. **15**, 539 (1970).
21. J. Miles, J. Fluid Mech. **79**, 157 (1977).
22. M. J. Ablowitz and H. Segur, *Solitons and the Inverse Scattering Transform*, Studies in Applied and Numerical Mathematics (SIAM, 1981).
23. Y. Kodama, J. Phys. A **37**, 11169 (2004).
24. Y. Kodama, J. Phys. A **43**, 434004 (2010).
25. W. Li, H. Yeh, and Y. Kodama, J. Fluid Mech. **672**, 326 (2011).
26. H. S. Eisenberg, Y. Silberberg, R. Morandotti, and J. S. Aitchison, Phys. Rev. Lett. **85**, 1863 (2000).
27. H. C. Yuen and B. M. Lake, Ann. Rev. Fluid Mech. **12**, 303 (1980).
28. D. Krokkel, N. J. Halas, G. Giuliani, and D. Grishkowsky, Phys. Rev. Lett. **60**, 29 (1988).
29. G. Biondini and Y. Kodama, J. Phys. A **36**, 10519 (2003).
30. P. K. Newton and J. B. Keller, SIAM J. Appl. Math. **47**, 959 (1987).
31. G. G. Luther, A. C. Newell, J. V. Moloney, and E. M. Wright, Opt. Lett. **19**, 789 (1994).
32. Y. Kominis, N. Moshonas, P. Papagiannis, K. Hizanidis, and D. N. Christodoulides, Opt. Lett. **30**, 2924 (2005).
33. K. Rypdal and J. J. Rasmussen, Phys. Scripta **40**, 192 (1989).
34. H. S. Eisenberg, R. Morandotti, Y. Silberberg, S. Bar-Ad, D. Ross, and J. S. Aitchison, Phys. Rev. Lett. **87**, 043902 (2001).
35. F. Baronio, C. De Angelis, P. Pioeger, V. Couderc, and A. Barthelemy, Opt. Lett. **29**, 986 (2004).
36. F. Baronio, C. De Angelis, M. Marangoni, C. Manzoni, R. Ramponi, and G. Cerullo, Opt. Express **14**, 4774 (2006).